Heat Transfer between Two Nanoparticles Through Near Field Interaction

Gilberto Domingues,[1,*] Sebastian Volz,[2,†] Karl Joulain,[1] and Jean-Jacques Greffet[2]

[1]*Laboratoire d'Etudes Thermiques, 86961 Futuroscope Cedex, France*

[2]*Laboratoire d'Energétique Macroscopique, Moléculaire; Combusion, Grande Voie des Vignes, Châtenay Malabry 92295, France*

(Received 23 July 2004; revised manuscript received 8 November 2004; published 2 March 2005)

We introduce a thermal conductance by using the fluctuation-dissipation theorem to analyze the heat transfer between two nanoparticles separated by a submicron distance. Using either a molecular dynamics technique or a model based on the Coulomb interaction between fluctuating dipoles, we derive the thermal conductance. Both models agree for distances larger than a few diameters. For separation distances smaller than the particle diameter, we find a transition regime characterized by a thermal conductance larger than the contact conductance.

DOI: 10.1103/PhysRevLett.94.085901 PACS numbers: 65.80.+n, 82.60.Qr

Understanding and predicting the heat transfer between two bodies separated by a nanometric distance is a key issue both from the theoretical and applied points of view. Most near-field techniques involve bringing a tip close to an interface. In many cases, the tip and the interface temperatures are not equal so that a heat transfer is generated. Superinsulating materials such as aerogels and highly conductive media such as nanofluids also involve heat exchanges between neighboring particles. However, there is a lack of understanding of the physical mechanisms involved. The heat transfer in quantum wells and at nanoscale has been analyzed in the context of phonon transport [1]. The heat transfer, through constrictions [2] or linear chains [3–5], has been discussed in many papers. The quantized thermal conductance has been studied both theoretically [6,7] and experimentally [8]. Yet all these works rely on the concept of phonon, which is hardly valid for small aggregates. Heat transfer between two planes separated by subwavelength distances through electromagnetic interaction has been first investigated by Polder and van Hove [9] and later by many groups [10,11]. It has been shown recently that this mechanism has a very large resonance at the optical phonon frequency for polar materials [12,13]. When the distance is decreased, the heat transfer increases dramatically.

A still open question is how energy is exchanged between two objects, a tip and a surface for instance, just before contact. The mechanisms involved are unclear. Whereas radiative heat transfer (i.e., emission and absorption of photons) is negligible, near-field radiation (i.e., Coulomb interaction) may become important. Dipole-dipole energy transfer also known as Forster energy transfer is the dominant energy transfer mechanism between molecules [14]. In this Letter, we explore the heat transfer between two nanoparticles (NPs) separated by a distance on the order of a few nanometers. We introduce a thermal conductance that can be related to the fluctuations of the heat flux using the fluctuation-dissipation theorem. We then implement a molecular dynamics simulation to compute the thermal conductance as a function of the separation distance. An alternative approach is based on a direct derivation of the heat flux between the two nanoparticles modeled by fluctuating dipoles. We find that both models agree and yield a $1/d^6$ dependence for distances larger than a few diameters. Yet when the distance is further decreased, we observe a stronger enhancement of the conductance followed by a decay when the NPs are in contact.

Let us first define the linear response susceptibility, relating the net heat flux Q_{12} exchanged between the two NPs to the NPs temperature difference:

$$\frac{Q_{12}(\omega)}{T_0} = G_{12}^*(\omega)\Delta T(\omega), \tag{1}$$

where T_0 is the mean temperature and ω is the circular frequency. The fluctuations of ΔT and Q_{12} are characterized by their power spectral densities $P_{\Delta T}$ and $P_{Q_{12}}$. When combining Eq. (1) with the definition of the power spectral density of a random stationary process X, $P_X(\omega) = \lim_{t\to\infty} \frac{1}{T}\langle |X_T(\omega)|^2\rangle$, where X_T is the Fourier transform of the restriction of $X_{(t)}$, to the finite time interval $[0, T]$, we obtain

$$P_{\Delta T}(\omega) = \frac{P_{Q_{12}}(\omega)}{|G_{12}^* T_0|^2}. \tag{2}$$

We now apply the fluctuation-dissipation theorem considering ΔT as the force and G_{12}^* as the susceptibility. The power spectral density of the temperature fluctuation is given by the fluctuation-dissipation theorem [15]:

$$P_{\Delta T}(\omega) = \frac{\mathrm{Re}(G_{12}^*)}{|G_{12}^*(\omega)|^2}\Theta(\omega, T_0), \tag{3}$$

where $\Theta(\omega, T_0)$ is the mean energy of an oscillator $\hbar\omega/(e^{h\omega/k_B T} - 1)$, and Re indicates the real part.

Combining Eqs. (2) and (3) yields

$$\mathrm{Re}[G_{12}^*(\omega)] = \frac{P_{Q_{12}}(\omega)}{T_0^2\Theta(\omega, T_0)}. \tag{4}$$

From Eq. (1), it is obvious that the thermal conductance

$G_{12} = Q_{12}/\Delta T$ is given by $G_{12} = T_0 G_{12}^*$. The static limit ($\omega = 0$) of Eq. (4) indicates that the time integration of the flux autocorrelation is directly proportional to the static thermal conductance. From the Wiener-Khinchin theorem, we have $P_{Q_{12}}(\omega) = \int_{-\infty}^{+\infty} \langle Q_{12}(0) Q_{12}(t) \rangle e^{-i\omega t} dt$, so that we need to compute the temporal fluctuation of the flux between the two silica NPs. To this aim, we use the molecular dynamics (MD) technique. It consists of computing all the atomic positions and velocities as a function of time. Each atom is modeled by a mass point whose trajectory is described by the second Newton's Law [16]:

$$\sum_j \mathbf{f}_{ij} = m_i \ddot{\mathbf{r}}_i, \tag{5}$$

where m_i and $\ddot{\mathbf{r}}_i$ are the atomic mass and acceleration, and $\mathbf{f}_{ij}$ represents the force exerted by atoms j on atom i. The interatomic forces describe the interaction in polar materials such as silica. They are derived from the van Beest, Kramer, and van Santen (BKS) interaction potential [17] in order to provide the full physical picture of the long range electromagnetic and the repulsive-attractive short range interactions. Accordingly, the BKS potential can be decomposed into a Coulomb and a Buckingham potential. The Buckingham part includes an exponential term to describe the repulsive forces and a sixth power term that represents the short range van der Waals attractive forces. The Coulomb potential takes into account the interatomic electrostatic forces. Neither a potential cutoff nor a limited neighbors list are implemented in the force calculation. No boundary conditions are applied. A fourth order Gear integration scheme [16] was used to provide the velocities $\mathbf{v}_i$ and the positions $\mathbf{r}_i$ from Eq. (5). The time step of 0.7 fs that is proposed in the literature [18] appears to be sufficiently small to ensure the total energy conservation. The simulation starts with two cubes of β-cristobalite crystals separated by a few nanometers. The two NPs are heated up during 2000 time steps to the same temperature $T_0 = 300$ K by using a conventional Gaussian thermostat. The β-cristobalite is not stable at this temperature so that the NPs lose their crystalline structure to become amorphous, as illustrated in Fig. 1. Since the NPs positions are not frozen, the van der Waals forces drive them to stick together. In order to avoid the artifacts due to the variation of the inter-NP distance, we stop the simulation when a 10% variation of the initial distance is reached. The error is reduced by computing several phase ensembles for the same macroscopic experiment. We also *a posteriori* checked that the heat transfer is characterized by a relaxation time much smaller than the physical simulation time. After the NPs have reached equilibrium, the exchanged power Q_{12} between the nanoparticle noted NP1 and the nanoparticle noted NP2 is computed as the net work done by a particle on the ions of the other particle (see Fig. 2):

$$Q_{12} = \sum_{\substack{i \in \mathrm{NP1} \\ j \in \mathrm{NP2}}} \mathbf{f}_{ij} \cdot \mathbf{v}_j - \sum_{\substack{i \in \mathrm{NP1} \\ j \in \mathrm{NP2}}} \mathbf{f}_{ji} \cdot \mathbf{v}_i. \tag{6}$$

To provide a basis for comparison, we also derive the spectral dissipated power $Q_{1\to 2}$ in NP2 due to the electromagnetic interaction NP1 in the framework of fluctuational electrodynamics [11]. The power at a given frequency can be expressed as a Joule term generated by a monochromatic field [11,12]:

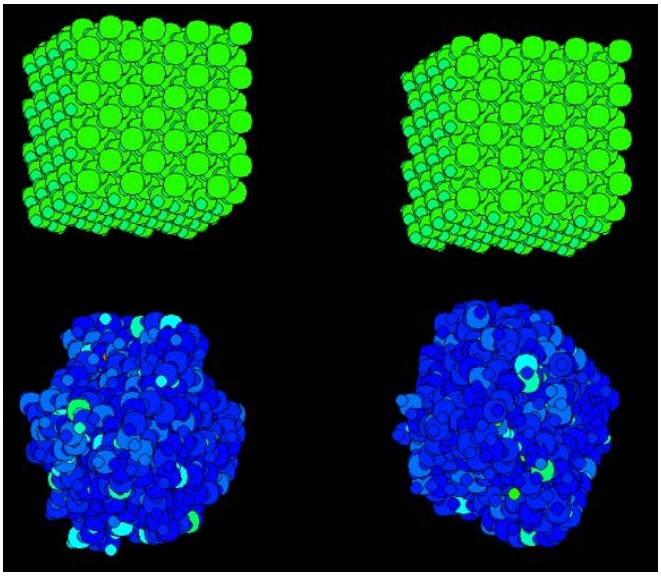

FIG. 1 (color online). Snapshots of the NPs at time $t = 0$ (top) and 1 ps after (bottom). The crystalline structure rapidly disappears and amorphous NPs are obtained. The color indicates the work done by the atom under the electrostatic field of the neighboring particle.

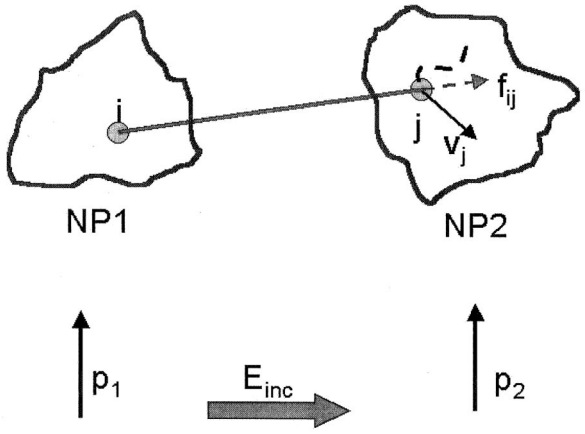

FIG. 2. Explanation schemes of the calculation of the power dissipated in the NP2 due to the field emitted by the NP1. In the MD computation (above), the power is computed as the work produced by the atomic motions of the NP2 atoms in the potential field generated by the NP1. In the electrostatic calculation (below), each NP is assimilated to one dipole (vectors $\mathbf{p}_1$ and $\mathbf{p}_2$) situated at the NP centers.

$$Q_{1\to 2}(\omega) = \frac{\omega\varepsilon_0}{2}\alpha_2''|\mathbf{E}_{\mathrm{inc}}(\mathbf{r}_2)|^2, \quad (7)$$

where α_2'' is the imaginary part of the NP2 polarizability. The modulus of the incident electric field is evaluated simply by using a dipole approximation. Because the separation distance d is smaller than the wavelength, retardation effects can be neglected so that an electrostatic approximation is valid. If in addition, $d \gg R$, where R stands for the effective radius of the particle, each particle is equivalent to a dipole. The incident field then takes the form $\mathbf{E}_{\mathrm{inc}} = \mathbf{G}\cdot\mathbf{p}$. $\mathbf{G}$ is the Green's dyadic given by $\mathbf{G} = \frac{1}{4\pi\varepsilon_0}\frac{1}{r^3}[\mathbf{1} - 3\mathbf{uu}]$, where $\mathbf{u}$ is the unit vector $\mathbf{r}/r$. Because of thermal fluctuations, each particle has a random electric dipole. The fluctuations-dissipation theorem yields the correlation function:

$$\langle p_k p_l\rangle = \frac{\varepsilon_0}{\pi\omega}\alpha_1''(\omega)\Theta(T_1,\omega)\delta(\omega-\omega')\delta_{kl}. \quad (8)$$

This equation yields α_1'' from a MD calculation of $\langle p_k p_l\rangle$. Using this result, and the form of the incident field produced by a dipole, we obtain

$$Q_{1\to 2} = \frac{3\alpha_1''\alpha_2''}{4\pi^3 d^6}\Theta(T_1,\omega). \quad (9)$$

The power exchanged between the NPs due to the dipole-dipole coupling can finally be written as [11]

$$Q_{12}(\omega) = \frac{3}{4\pi^3}\frac{\alpha_1''(\omega)\alpha_2''(\omega)}{d^6}[\Theta(\omega,T_1) - \Theta(\omega,T_2)]. \quad (10)$$

This is drastically different from the usual radiative heat transfer flux due to the emission and absorption of photons in the far field [11]:

$$Q_{12}^{\mathrm{FF}}(\omega) = \frac{\omega^4\alpha_1''(\omega)\alpha_2''(\omega)}{32\pi^3 c^4 d^2}[\Theta(\omega,T_1) - \Theta(\omega,T_2)], \quad (11)$$

where c is the light velocity. We can linearize Eq. (10) to obtain the following form of the conductance:

$$G_{12}(T_0) = \frac{3}{4\pi^3}\int_0^\infty \Theta'(\omega,T_0)\alpha_1''(\omega)\alpha_2''(\omega)d\omega\frac{1}{d^6}, \quad (12)$$

where Θ' is the temperature derivative of the function Θ. The near-field and far-field contributions have the same order of magnitude when $d = 2\pi c/\omega$, but the dipole-dipole heat transfer is 12 orders of magnitude larger when $d = 10$ nm. In silica, the main contributions to the integral in Eq. (11) are the resonant phonon-polariton modes with frequencies equal to 20 and 33 THz . They appear as sharp peaks in the polarizability spectrum and therefore in the spectrum of the exchanged power. The polarizability is proportional to the NP volume and G_{12} is proportional to the product $\alpha_1''\alpha_2''$, so that the conductance should increase as the effective radius R to the power six. Equation (11) also provides the conductance dependence on the interparticle distance $d = |r_2 - r_1|$ as a d^{-6} law. The field produced by a dipole in the near field at a distance d is proportional to d^{-3}. It follows that the exchanged power is linearly dependent to d^{-6}. In Fig. 3, the thermal conductances are reported as a function of the internanoparticle distance. In the distance interval (8–100 nm), the MD (data points) and the dipole-dipole (thick lines) models are in very good agreement. This constitutes a validation of the molecular dynamics based near-field analysis and also shows that the polarizability is relevant up to nanometric sizes. At distances smaller than 8 nm (4 diameters), a deviation between the MD and the dipole-dipole model appears. This deviation reaches 4 orders of magnitude as compared to the dipole-dipole model. In order to understand the origin of the enhanced heat transfer, we have studied the contribution of the Buckingham potential which is not taken into account in the dipole-dipole model. We have evaluated separately the contributions of the three terms of the potential: repulsive and attractive parts of the Buckingham potential and Coulomb potential. The latter always dominate the transfer in the range of investigation. Thus, the increase of the conductance cannot be attributed to short range interactions. It appears to be due to the contribution of multipolar Coulomb interactions. Indeed, the field produced by a particle cannot be considered as uniform in the neighboring particle when the separation distance is on the order of the NP's diameter. This explanation is supported by Fig. 3. It is clearly seen that the deviation between both models

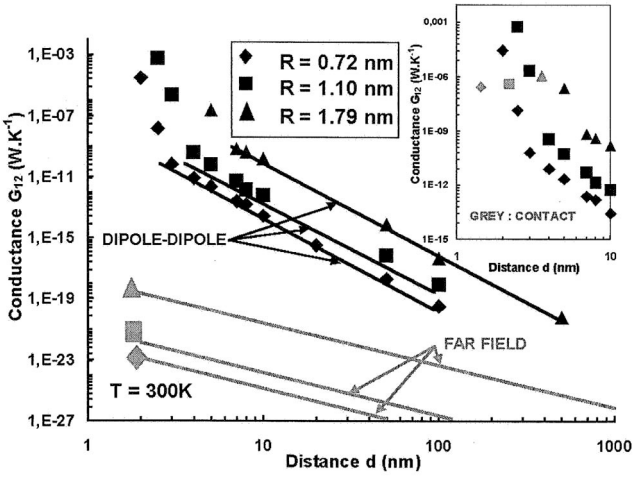

FIG. 3. Thermal conductance G_{12} vs distance d between the centers of mass. R corresponds to the nanoparticle radius and N is the number of atoms in each particle. While the MD (data points) and the analytical (thick lines) predictions agree very well when the interparticle distance is larger than the nanoparticle diameter, a deviation appears when $d < 4R$. The far-field conductance due to emission and absorption is reported for comparison. The inset highlights the conductance values when the NPs are in contact (gray data points). Their abscissa correspond to $2R$. The contact conductance is 2 to 3 orders of magnitude lower than the conductance just before contact.

occurs for a distance between particles which is between $4R$ and $5R$ for the three cases studied. These results show that the thermal conductance increases continuously when the distance between NPs is decreased. It entails that the strong coupling between the particles is responsible for a transition regime between far-field radiation and conduction.

We also have done calculations of the conductance when the particles are in contact. Surprisingly, we find that the contact conductance is smaller than the conductance for a separation distance of the order of the particle radius as seen in the insert of Fig. 3 for the two smallest particles. Since the Buckingham contribution is negligible before contact, the conductance is only due to the autocorrelation of the Coulomb power $\langle {Q_{12}}^{\mathrm{C}} {Q_{12}}^{\mathrm{C}}(t)\rangle$. At contact, this last quantity does not vary much but three other terms appear: the pure Buckingham contribution $\langle {Q_{12}}^{\mathrm{B}} {Q_{12}}^{\mathrm{B}}(t)\rangle$ and the cross terms $\langle {Q_{12}}^{\mathrm{C}} {Q_{12}}^{\mathrm{B}}(t)\rangle$ and $\langle {Q_{12}}^{\mathrm{B}} {Q_{12}}^{\mathrm{C}}(t)\rangle$. The calculation shows that the cross terms are negative and on the order of $\langle {Q_{12}}^{\mathrm{B}} {Q_{12}}^{\mathrm{B}}(t)\rangle$. Therefore the final sum is lower than $\langle {Q_{12}}^{\mathrm{C}} {Q_{12}}^{\mathrm{C}}(t)\rangle$. The origin of this decay is still an open question. It might be possible that the contact produces a correlation of the positions of the atoms of both particles that results in a smaller fluctuation of Q_{12}.

One can speculate on the properties of a chain of particles. It has been shown recently [20] that a chain of metallic particles can be used as a waveguide of electromagnetic energy due to the coupling of surface plasmons between neighboring particles. We have found that a similar coupling involving localized polaritons is responsible for the heat transfer at small distances. These results suggest that the thermal conductance of a chain of particles might be larger than the conductance of a continuous rod.

In conclusion, we have reported an analysis of heat transfer between two nanoparticles as a function of their separation distance. We have used a MD technique and the fluctuation-dissipation theorem to compute the thermal conductance between two nanoparticles. We have also introduced a model based on a dipole-dipole interaction. Both models agree for distances larger than 2 diameters. In all cases, the Coulomb potential and the resonant excitation of the polariton modes are responsible for the large heat transfer. At separation distances smaller than the diameter, the heat transfer due to multipolar contributions is enhanced by several orders of magnitude. The heat transfer before mechanical contact is found to be 2 to 3 orders of magnitude more efficient than when the NPs are in contact. These results show that the traditional separation between conduction and radiation is no longer meaningful at these length scales.

S. V. acknowledges a Grant from the French Commissariat à L'Energie Atomique (CEA).

*Electronic address: gilberto.domingues@let.ensma.fr
†Electronic address: volz@em2c.ecp.fr

[1] G. Chen, Phys. Rev. B **57**, 14958 (1998).
[2] K. R. Patton and M. R. Geller, Phys. Rev. B **64**, 155320 (2001).
[3] A. Dhar, Phys. Rev. Lett. **86**, 5882 (2001).
[4] P. L. Garrido, P. I. Hurtado, and B. Nadrowski, Phys. Rev. Lett. **86**, 5486 (2001).
[5] A. Ozpineci and S. Ciraci, Phys. Rev. B **63**, 125415 (2001).
[6] L. G. C. Rego and G. Kirczenow, Phys. Rev. Lett. **81**, 232 (1998).
[7] T. Yamamoto, S. Watanabe, and K. Watanabe, Phys. Rev. Lett. **92**, 75502 (2004).
[8] K. Schwab, E. A. Henrlksen, J. M. Worlock, and M. L. Roukes, Nature (London) **404**, 974 (2000).
[9] D. Polder and M. van Hove, Phys. Rev. B **4**, 3303 (1971).
[10] J. B. Pendry, J. Phys. Condens. Matter **11**, 6621 (1999); J. J. Loomis and H. J. Maris, Phys. Rev. B **50**, 18517 (1994); A. Narayanaswamy and G. Chen, Appl. Phys. Lett. **82**, 3544 (2003).
[11] A. I. Volokitin and B. N. J. Persson, Phys. Rev. B **63**, 205404 (2001).
[12] J.-P. Mulet, K. Joulain, R. Carminati, and J.-J. Greffet, Appl. Phys. Lett. **78**, 2931 (2001).
[13] J.-P. Mulet, K. Joulain, R. Carminati, and J.-J. Greffet, Microscale Thermophysical Engineering **6**, 209 (2002).
[14] Th. Förster, Ann. Phys. (Berlin) **2**, 55 (1948).
[15] H. B. Callen and T. A. Welton, Phys. Rev. **83**, 1 (1951).
[16] M. P. Allen and D. J. Tildesley, *Computer Simulation of Liquids* (Oxford University Press, New York, 1987).
[17] B. W. H. van Beest, G. J. Kramer, and R. A. van Santen, Phys. Rev. Lett. **64**, 1955 (1990).
[18] S. Volz, Phys. Rev. Lett. **87**, 74301 (2001).
[19] G. Domingues, J.-B. Saulnier, and S. Volz, Superlattices Microstruct. (to be published).
[20] S. A. Maier *et al.*, Nat. Mater. **2**, 229 (2003).